

FINITE ELEMENT THREE-DIMENSIONAL ELASTIC-PLASTIC CREEP ANALYSIS

A. LEVY

*Research Department, Grumman Aerospace Corporation,
Bethpage, New York 11714, U.S.A.*

This paper presents a continued development of computationally efficient finite-element methods for accurately predicting the isothermal three-dimensional elastic-plastic creep responses of thick and thin shell structures subjected to mechanical and thermal loads. This work is directed toward verifying the structural integrity of liquid metal fast breeder reactor (LMFBR) components in the creep regime.

Previous work in this area for elastic-plastic analysis was demonstrated by Levy, Pifko, and Armen (see paper L4/4; SMiRT 4). In this reference, use of optimal stress points as well as a variable number of stress points within an element allowed the monitoring of the stress history at many points within that element. These ideas have been extended for combined plasticity and creep behavior. Thus, within an element, the order of the allowable total kinematic strain variation is dependent on the number of element nodes, and the order of the allowable plastic strain variation (and hence the elastic-plastic boundaries) and/or creep strain variation is dependent on the number of stress points. This allows for an accurate representation of the elastic-plastic creep behavior within an element. This higher inelastic representation results in the use of a minimum number of degrees of freedom for a given nonlinear analysis, which is particularly important for combined creep and plasticity behavior and for cyclic loading, where computer times can be prohibitive.

The basic numerical solution procedure for the elastic-plastic creep analysis is an incremental predictor-corrector iterative scheme combined with the 'initial strain' approach. Attention has been given to the time step increment strategy for combined plasticity and creep as this governs efficiency and accuracy.

These methods have been implemented into the three-dimensional solid element module (HEX) of the Grumman PLANS finite element program.

Sample problems are used to demonstrate and investigate the accuracy and efficiency of these methods. Sample problems include combined plasticity and creep analysis of a simple rod under time varying load, stress-relaxation of a simple rod, thermal stress-relaxation of a plate subjected to a temperature variation across the width, and creep analysis of an internally loaded thick-walled pressure vessel.

1. Introduction

The use of accurate and efficient finite-element methods for the analysis of isothermal three-dimensional elastic-plastic creep behavior due to mechanical and thermal loadings is incorporated into the three-dimensional solid element module (HEX) of the Grumman PLANS finite element programs for nonlinear analysis [1, 2]. These methods include an incremental formulation based on the 'initial strain' concept as described by Armen et al. [1] for the elastic-plastic formulation. The basic numerical solution procedure for the elastic-plastic creep analysis is a predictor-corrector iterative scheme combined with the 'initial strain' approach. This scheme is an extension of an iterative procedure for creep outlined by Mendelson, Hirschberg, and Mason [3], and modified by Dahl [4]. Within this procedure three subprocedures are described, each of which is most accurate and efficient for different classes of problems.

Much attention has been given to the time step increment strategy for combined plasticity and creep as this governs efficiency and accuracy. These considerations have led to a strategy based on the work of Zienkiewicz and Cormean [5]. Also included is a set of auxiliary rules for stress reversal conditions similar to those outlined by Corum et al. in ref. [6].

Previous work for elastic-plastic analysis was demonstrated by Levy, Pifko, and Armen [7]. In this reference, use of optimal stress points as well as a variable number of stress points within an element allowed the monitoring of the stress history at many points within that element. These ideas have been extended for combined plasticity and creep behavior. Thus, within an element, the order of the allowable total kinematic strain variation is dependent on the number of element nodes, and the order of the allowable plastic strain variation (and hence the elastic-plastic boundaries) and/or creep strain variation is dependent on the number of stress points. This allows for an accurate representation of the elastic-plastic creep behavior within an element. This higher order inelastic representation results in the use of a minimum number of degrees of freedom for a given nonlinear analysis, which is particularly important for combined creep and plasticity behavior or for cyclic loading, where computer times can be prohibitive.

Sampling problems are used to demonstrate and investigate the accuracy and efficiency of these methods. Sample problems include combined plasticity and creep analysis of a simple rod under time varying load, stress-relaxation of a simple rod, thermal stress-relaxation of a plate subjected to a temperature variation across the width, and creep analysis of an internally loaded thick-walled pressure vessel.

2. Description of HEX Finite Element Program

2.1 Description of Elastic-Plastic Creep Methods

The incremental matrix equation using the initial strain concept as outlined in [1] is extended to include creep as follows:

$$[K] \{\Delta u\}_i = \{\Delta P\}_i + \{R\}_i + \{\Delta P_p\}_{i-i} + \{\Delta P_c^{PR}\}_i \quad (1)$$

where

- $[K]$ = conventional stiffness matrix in terms of elastic properties
- $\{\Delta u\}_i$ = incremental displacement at the i th step
- $\{\Delta P\}_i$ = incremental external load at the i th step
- $\{R\}_i$ = equilibrium correction at the i th step to alleviate any drifting from equilibrium state as a result of the incremental linearization procedure
- $\{\Delta P_p\}_{i-1}$ = effective incremental load vector based on the change in plastic strain at the $(i-1)$ th step, and
- $\{\Delta P_c\}_i$ = predicted effective incremental load vector based on the change in creep strain at the i th step

2.1.1 Plasticity

As part of the initial strain method the stiffness matrix need never be reformed after the first increment since the nonlinearities appear as an added component to the load vector. Consequently, the stiffness matrix is factored only once for an entire analysis. Since the exact values of the plastic strain increments for the i th step are not known, use is made of the estimated values taken from the $(i - 1)$ th step in $\{\Delta P_p\}_{i-1}$ as denoted in eq.(1). This incremental procedure can lead to a drifting from total equilibrium. This is corrected for by the use of the equilibrium correction term, $\{R\}_i$ in eq.(1), based on the total equilibrium at the end of the current load step.

The elements of the effective load vector depend on the current state of stress, yield criterion, flow rule and hardening law. Hill's yield criterion [8] for an orthotropic material, which reduces the Von Mises yield condition for isotropic material, is used to predict initial yield and to obtain the flow rules of plasticity. The hardening law is based on the Prager-Ziegler kinematic hardening theory [9] modified for orthotropic material behavior. Elastic ideally plastic, linear strain hardening, and nonlinear strain hardening options are available. Proportional and nonproportional cyclic loading conditions are allowed. For a detailed description of the complete elastic-plastic cyclic theory used in the PLANS program see refs. [1] and [2].

2.1.2 Combined Plasticity and Creep

A flow diagram representing these procedures is presented in Fig. 1. The method used for the numerical procedure is a predictor-corrector iterative scheme. This scheme is an extension of an iterative procedure for creep outlined in [3] and modified in [4]. The effective incremental load in eq.(1) can be represented as

$$\{\Delta P_c^{PR}\}_i = [K^*] \{(\Delta \epsilon_{ij}^c)^{PR}\}_i$$

where

$[K^*]$ = initial strain matrix

$(\Delta \epsilon_{ij}^c)^{PR}$ = predicted incremental creep strain components for i th step

The predicted equivalent incremental creep strains, $\Delta \bar{\epsilon}^c$, found from the $\Delta \epsilon_{ij}^c$, are compared to the resulting values at the end of the i th step. If the comparison is unfavorable

(no convergence), a new set of predicted equivalent incremental creep strains is found for and the time step is repeated. This is continued until convergence occurs. Within this procedure three different options are available, these are:

1. Basic predictor-corrector iterative procedure as shown in flow diagram
2. Predictor-corrector procedure, i.e., no iteration takes place as the solution marches forward
3. Same as 1, except no predictor solution is used

Each of these procedures is most practical for certain classes of problems. Method 2 is the fastest and most practical when stress relaxation does not occur. Also, if approximate answers are required this method is excellent. Methods 1 and 3 are practically identical. For highly nonlinear regions, method 1 appears to be the most efficient, otherwise method 3 appears to be best.

The creep behavior is accounted for by incorporating the following key features:

2.1.2.1 Uniaxial Creep Law

A uniaxial "creep law" describes the experimental uniaxial constant-stress, isothermal creep curves. Two basic forms are allowed.

$$\epsilon^c(\sigma, \tau) = f(\sigma) [1 - e^{-r(\sigma)\tau}] + g(\sigma)\tau \quad (2)$$

$$\epsilon^c(\sigma, \tau) = \beta(\sigma) t^{q(\sigma)} + k(\sigma)\tau$$

where f , r , g , β , q and k are functions of stress

τ = "material time"

ϵ^c = creep strain

σ = stress

For multiaxial cases, eq. (2) is generalized by replacing σ by $\bar{\sigma}$ (equivalent stress) and ϵ^c by $\bar{\epsilon}^c$ (equivalent strain). The coefficients may be expressed as power of stress, e.g., $f(\bar{\sigma}) = F\bar{\sigma}^m$, or in tabular form. Also, the user may specify the equivalent creep strain above which only secondary creep applies.

2.1.2.2 Flow Rule

The flow rule is based on proportionality between creep strain rate components and deviatoric stresses, (as in the Prandtl-Reuss flow rule in plasticity), expressed as

$$\dot{\epsilon}_{ij}^c = \frac{3}{2} \frac{\dot{\bar{\epsilon}}^c(\bar{\sigma}, \bar{\epsilon}^c)}{\bar{\sigma}} \sigma'_{ij} \quad (3)$$

where σ'_{ij} = deviatoric stress

$\bar{\epsilon}^c$ = equivalent total creep strain

$\dot{\bar{\epsilon}}^c$ = equivalent total creep strain rate

2.1.2.3 Strain-Hardening Rule

The strain-hardening rule assumes that in going from one stress level to the next the equivalent creep rate expressed eq. (3) depends on the existing equivalent creep strain as well as stress.

2.1.2.4 Auxiliary Rules

A set of auxiliary rules is used for stress reversal conditions. For a multiaxial state, a stress reversal is considered to occur whenever the effective creep strain measured from the current origin begins to change direction. The rule takes the form

$$\dot{\epsilon}_{ij}^c = \lambda (\bar{\sigma}, \bar{\epsilon}^H) \sigma_{ij}^i \quad (4)$$

where $\bar{\epsilon}^H$ is the current value of strain hardening, which may differ from $\bar{\epsilon}^c$. The methods incorporated into the program to account for stress reversals are based on those outlined in ref. [10].

2.1.2.5 Automatic Time Adjustment

An automatic time adjustment scheme is incorporated. The time step is always kept within certain bounds. If the time step is too large, instability occurs (at best, accuracy is poor as it is difficult to follow the time history precisely). If the time step is too small, the expense of solving a problem is very high. The criterion for time step selection follows those outlined in [5]. Here the time step is based on total strain for stability and accuracy, as follows

$$\Delta T < \tau \bar{\epsilon}_{total} / \dot{\epsilon}^c \quad (5)$$

where $\bar{\epsilon}_{total}$ is the effective total strain.

In general, values of the admissibility constant τ in the range 0.1 to 0.15 are effective for 'contained' problems but much lower values are needed near collapse. Zienkiewicz and Corneau [5] suggest values in this range of 0.01 to 0.05. A time step can also be increased for a maximum factor equal to 1.5 times the old time step. A limit of 1.5 increase in the time step is also suggested in ref. [5]. The user can specify different admissibility criteria in different ranges of total creep strain or total time. In addition, the time step is controlled by the amount of incremental plastic strain, such that

$$\Delta \bar{\epsilon}^p < \eta \bar{\epsilon}_{total}$$

where $\Delta \bar{\epsilon}^p$ is the effective incremental plastic strain.

2.2 Description of Isoparametric Solid Element

The basic finite element used is an isoparametric solid element as described by Zienkiewicz et al. [11]. A variable number of nodes of between eight and twenty are allowed for each element as described by Levy [12]. In practice this variable node feature is especially useful when a mesh changes character, e.g. going from a coarser to a finer mesh. It is also applicable to problems in which the mechanical behavior is directional, e.g. when bending is significant in one direction and shear deformation is significant in another. The use of this 'variable node' isoparametric element allows the user to specify the number of nodes contained in an element without resorting to external methods such as constraint equations, which may be costly.

2.3 Use of Multistress Points

The use of multistress points within an element has been incorporated into the program. This allows a monitoring of the stress and strain history of a number of points within each element. The number of stress points can be chosen independently from the order of the element displacement function. Thus, within an element, the order of the allowable total kinematic strain variation is dependent on the number of element nodes; and the order of the allowable plastic strain variation (and hence the elastic-plastic boundaries) and creep strain variation is dependent on the number of stress points and the accuracy of the total kinematic strain variation. Either Gauss or Lobatto points (in which boundary points are included in the set) can be specified within each element, and each element can be specified differently. Lobatto points are of particular importance where it is necessary to detect initial and subsequent yielding on a surface. Optimal stress points [13] are also included. This is an array of Gauss points one order lower in each direction than that needed to represent the element displacement distribution (or to integrate its stiffness). At these points the stresses are as accurate as the nodal displacements. A plate with a steady state temperature distribution across its width is used to demonstrate the use of multistress points in a creep analysis.

2.4 Other Program Features

2.4.1 Thermal Load

Rather than using average element temperatures in a thermal analysis the temperature is allowed to vary within an element. The order of the temperature variation is assumed to be the same as the element displacement variation. This is incorporated into the thermal load vector. Thus, for a 20-node element a quadratic temperature distribution, within an element, can be described exactly. Also the thermal strains and corresponding stresses computed at stress points utilize the stress point temperatures, which are found from the same temperature distribution used in calculating the load vector. Thus, there is a compatibility between the formulation of the thermal load and thermal strains.

2.4.2 Restart

Since inelastic deformation is a path-dependent process, a restart capability is an important feature in large analyses, allowing the user to examine the deformation history to some intermediate load level before proceeding further in the analysis. The restart procedure incorporates some special features that are useful for load cycling. During an initial load-time history, restart information can be saved at a number of load-time points along the way. The user can then restart the computations at any of these intermediate points by either unloading from a given point in the load history to calculate residual stresses and strains or begin a load reversal to examine a cyclic loading history.

3. Sample Problems

Sample problems are presented to demonstrate the current methods and act as a guide for future problem solving.

3.1 Uniaxial Extension of a Rod With a Varying Time Load-Combined Creep and Plasticity

A uniform load is applied to the ends of a rod as shown in Fig. 2. The load amplitude varies in time as $P = 10^5 \cdot (2 + 0.1t)$ and the stress-strain curve is assumed bilinear, as shown, with a yield stress of 175,000 psi and a tangent modulus of $E/4$. Secondary creep is assumed with a creep law as follows,

$$\dot{\epsilon}^c = 3 \times 10^{-26} \sigma^4 \operatorname{sgn}(\sigma). \quad (6)$$

The corrector-iterative method (method 3 as outlined in Section 2.1.2) is used, and the results are shown in Fig. 3. The stress and plastic strains agree almost exactly with predicted results, while the creep strain differs from the predicted values, the difference depending on the admissibility constant used. This difference is shown in Fig. 4 as a percentage of total strain for different admissibility constants, τ . As found in ref. [5], using a value of $\tau < 0.15$ yields accurate and stable results. For $\tau = 0.2$, the problem becomes unstable after 60 hours. In the stable range, the error in creep strain varies approximately linearly with τ . For this problem the noniterative predictor-corrector procedure gives results at least as accurate as those shown for the corrector-iterative method and the error in creep strain does not vary with τ .

3.2 Stress Relaxation of a Rod - Creep Only

The stress relaxation of a rod under secondary creep, described by the creep law

$$\dot{\epsilon}^c = 3 \times 10^{-26} \sigma^4 \operatorname{sgn}(\sigma) \quad (7)$$

is investigated. The rod is strained to $\epsilon_f = 0.01$ in. and held for 600 hours. Figure 5 represents the results for a single element idealization. The solution can be found by substituting

$$\sigma = E(\epsilon_f - \epsilon^c) \quad (8)$$

into eq. (7), yielding

$$\frac{d\epsilon^c}{(\epsilon_f - \epsilon^c)^4} = 3 \times 10^{-26} E^4 dt \quad (9)$$

which can be integrated directly, and substituted into eq. (8), resulting in

$$\sigma = \left[\frac{1/3}{3 \times 10^{-26} E^4 t + 1/3 \epsilon_f^3} \right]^{1/3}. \quad (10)$$

Setting the admissibility constant $\tau = 0.15$, the finite element solution, using method 3, agrees exactly with the theoretical solution. For the noniterative predictor-corrector method (method 2 as outlined in Section 2.1.2), the solution diverges from the exact solution as the admissibility constant increases; i.e., as the time step increases. For an admissibility constant of 0.10, the average error in stress over the history of response is approximately 15 percent. This error is reduced to 5 percent for $\tau = 0.05$ and 1 percent for $\tau =$

0.01. The computer cost using method 2 with $\tau = 0.01$ (error 1 percent) is approximately 75 percent of that using method 3 with $\tau = 0.15$, and the computer cost using method 2 with $\tau = 0.05$ (error 5 percent) is approximately 25 percent of that using method 3 with $\tau = 0.15$.

3.3 Thermal Stress Relaxation - Creep Only

An infinite plate of width $2c$ is subjected to a steady state temperature distribution across the width, as shown in Fig. 6a. Secondary creep is assumed with the creep rate given as

$$\dot{\epsilon}^c = 3 \times 10^{-24} \sigma^4 \text{sgn}(\sigma) \quad (11)$$

Unlike the stress relaxation of a rod discussed earlier, no closed form solution exists. Similarly to the previous problem, the solution can be found by substituting

$$\sigma = E(\epsilon - \epsilon^c) \quad (12)$$

into eq. (11), yielding

$$\frac{d\epsilon^c}{(\epsilon - \epsilon^c)^4} = 3 \times 10^{-24} E^4 dt \quad (13)$$

along with

$$\epsilon = -0.0057(y^2 - 1/3) + \int_0^1 \epsilon^c dy \quad (14)$$

where $\epsilon = \epsilon_x - \alpha T$.

If ϵ were constant, then eq. (13) would be the stress relaxation equation found in the previous sample problem, eq. (9), and be integrable directly. As it is, a numerical procedure must be used to integrate eqs. (13) and (14), but this procedure can be the same as that used in the finite element solution.

The finite element solution is found for various Lobatto point schemes across the width. The creep strain distribution at $t = 100$ hr is shown in Fig. 6b, and the stress relaxation is shown in Fig. 6c. As the number of Lobatto points is increased across the width, the creep strain profile is represented more accurately, resulting in a better approximation of the integration performed in eq. (14). A single twenty node element is sufficient to represent the exact elastic and thermal strains. The inelastic part of the total strain is found to be more accurate as the number of stress (strain) integration points are increased and does not require any finer finite element idealization. This is equivalent to stating that the integral of creep strain in eq. (14) is more accurate as the number of integration points (or stress points) is increased. Seven Lobatto points appear to be sufficient for this problem as the solution is within 0.5 percent of the solution using 17 Lobatto points (9 Lobatto points across half the width). Thus, an accurate representation of the creep strain distribution within an element can be obtained with the use of multistress points, eliminating the need for a finer idealization.

3.4 Internally Loaded Thick-Walled Cylinder - Creep Only

A thick-walled cylinder is subjected to a uniform internal pressure of 365 psi. Figure 7 shows the finite element idealization which consists of ten 20-node elements. Here a slice

is cut out of the cylinder and axisymmetric boundary conditions applied. Secondary creep is assumed with the creep strain rate given as

$$\dot{\epsilon}^c = 6.4 \times 10^{-18} \bar{\sigma}^{-4.4}$$

where $\bar{\epsilon}^c$ and $\bar{\sigma}$ correspond to the equivalent creep strain and equivalent stress, respectively. Figure 8 shows the stress-time history at the inner and outer radii of the cylinder. Steady state is reached after approximately 20 hours. This does not agree with the results found in ref. [14] where steady state is reached after two hours. It is conjectured that their results may have been misplotted. Figure 9 represents the stress components at steady state which are compared to the exact solution as given in ref. [15]. Optimal stress points are used in the finite element solution. The results agree almost exactly with theory. This model was also used to compare the HEX program with the solutions to other programs. Reference [16] compares the solution for an internal pressure of 3650 psi and a more complex creep law. The HEX results agree very closely with the average results shown in ref. [15].

4. Conclusions

The HEX program is capable of analyzing three-dimensional elastic-plastic creep behavior of thick and thin shell structures under combined mechanical and thermal loading.

The use of multistress and optimal stress points to accurately and efficiently predict the creep strain distribution through an element has been shown.

The use of a predictor-corrector iterative scheme for combined elastic-plastic creep behavior has been demonstrated. In general, the corrector iterative scheme is best, but for problems with a minimum of stress relaxation or stress redistribution, or where an approximate solution is sufficient, the predictor-corrector noniterative scheme is most efficient. In general, an admissibility constant of 0.05, indicating a time step limited to that which will yield an incremental creep strain of 5 percent of the total strain, is necessary in order to limit the solution error to 2 percent.

5. Application in Progress

The program is currently being used to predict the elastic-plastic creep behavior of a cylindrical nozzle-toroidal fillet-spherical shell representing a scaled test model of a LMFBR inlet nozzle. This problem has previously been investigated in the elastic-plastic range [7, 17].

6. Acknowledgement

The author gratefully acknowledges the contributions of Dr. Allan Pifko for his helpful insights and dedicated help in finite-element methodology and for his assistance in programming key portions of the PLANS code, Dr. Harry Armen, Jr. for his helpful insights into creep behavior and associated inelastic finite element algorithms and methods, and Patricia Ogilvie of Grumman Data Systems for programming portions of the PLANS code.

This work was partially supported by the Department of Energy through Oak Ridge National Laboratory.

Reference

- [1] Armen, H. Jr., Levine, H.S., Pifko, A., and Levy, A., "Nonlinear Analysis of Structures," NASA CR-2351, March 1974.
- [2] Pifko, A., Levine, H.S., Armen, H. Jr., and Levy, A., "PLANS - A Finite Element Program for Nonlinear Analysis of Structure," ASME Preprint 74-WA/PVP-6, presented at the ASME Winter Annual Meeting, New York, November 17-22, 1974.
- [3] Mendelson, A., Hirshberg, M.H., and Manson, S.S., "A General Approach to the Practical Solution of Creep Problems," J. of Basic Engineering, pp. 585-593, December 1959.
- [4] Dahl, N.C., Discussion of Mendelson's paper, J. of Basic Engineering, p. 595, December 1959.
- [5] Zienkiewicz, O.C., and Corneau, J.C., "Visco-Plasticity - Plasticity and Creep in Elastic Solids -- A Unified Numerical Solution Approach," International J. for Numerical Methods in Engineering, Vol 8, pp. 821-845, 1974.
- [6] Corum, J.M., Greenstreet, W.L., Liu, K.C., Pugh, C.E., and Swindeman, R.W., "Interim Guidelines for Detailed Inelastic Analysis of High-Temperature Reactor System Components," Oak Ridge National Laboratory Report ORNL-5014, December 1974.
- [7] Levy, A., Pifko, A., and Armen, H. Jr., "Finite Element Elastic-Plastic Analysis of LMFBR Components," Nuclear Engineering and Design, Vol. 45, No. 2, pp. 411-418, February 1978, also paper L4/4 presented at the 4th International Conference on Structural Mechanics in Reactor Technology, San Francisco, California, August 15-19, 1977.
- [8] Hill, R., The Mathematical Theory of Plasticity, Oxford University Press, 1950, Chapter 12.
- [9] Ziegler, H., "A Modification of Analyzing Stress and Strains in Work-Hardening Plastic Solids," J. Appl. Mech., Vol. 23, p. 493, 1956.
- [10] Corum, J.M., Greenstreet, W.L., Liu, K.C., Pugh C.E., and Swindeman, R.W., "Interim Guidelines for Detailed Inelastic Analysis of High-Temperature Reactor System Components," Oak Ridge National Laboratory Report ORNL-5014, December 1974.
- [11] Zienkiewicz, O.C., Irons, J.E., Admad, S., and Scott, F.C., "Isoparametric and Associated Element Families for Two and Three Dimensional Analysis," Proc. Finite Element Methods Stress Analysis, I. Holand and K. Bell, Eds., Tapir, pp. 383-434, 1969.
- [12] Levy, A., "A Three Dimensional 'Variable Node' Isoparametric Solid Element," Grumman Research Department Memorandum RM-587, July 1974.
- [13] Barlow, J., "Optimal Stress Locations in Finite Element Models," International J. of Numerical Methods in Engineering, Vol. 10, pp. 243-251, 1976.
- [14] Greenbaum, G.A., "Creep Analysis of Axisymmetric Bodies Using Finite Elements," Nuclear Engineering and Design, Vol. 7. pp. 379-397, 1968.
- [15] Odquist, F.K.G., and Hult, J, Kriechfestigkeit Metallischer Werkstoffe, Springer-Verlag, Berlin, Gottingen, Heidelberg, pp. 122-128, 1962.
- [16] Clinard, J.A., McKinley, D.A., Kroenke, W.C., and Sartory, W.K., "Verification by Comparison of Independent Computer Program Solutions," Pressure Vessels and Piping Computer Program Evaluation and Qualification, PVP-PB-024, in connection with The Energy Technology Conference, Houston, Texas, September 18-23, 1977.
- [17] Levy, A., Pifko, A., and Armen, H., Jr., "Development and Application of the PLANS Computer Program for Analysis of Nuclear Reactor Structural Components," ORNL/SUB/4485-1, Grumman Research Department Report RE-542, June 1977.

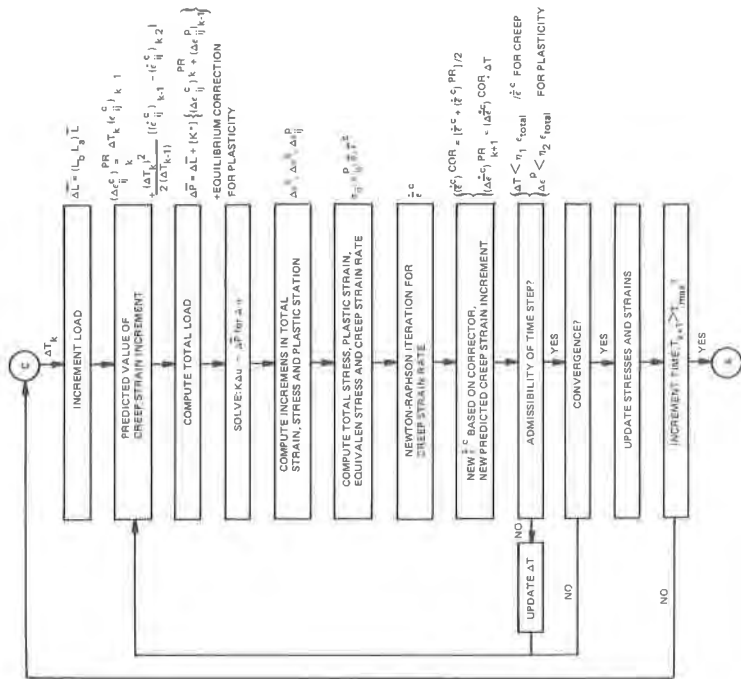
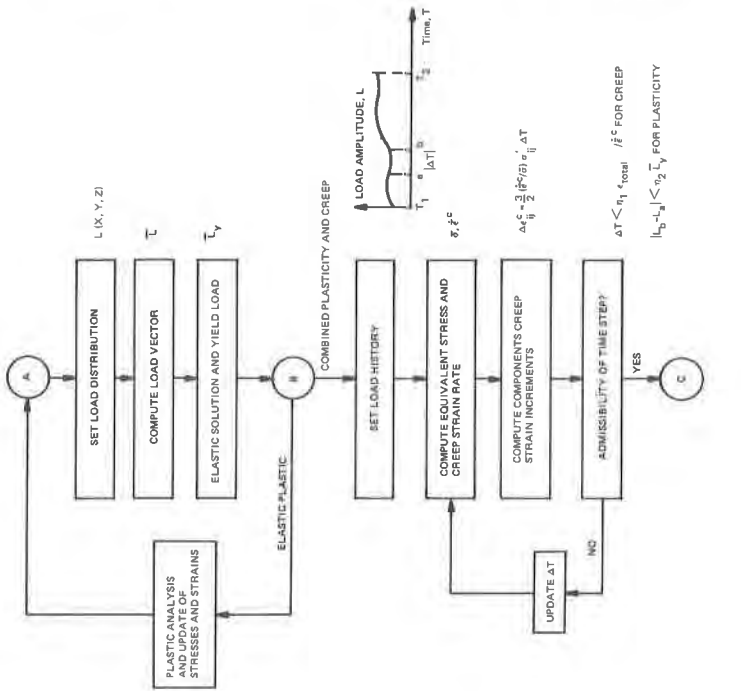


Fig. 1 - Flow Diagram for Combined Plasticity and Creep

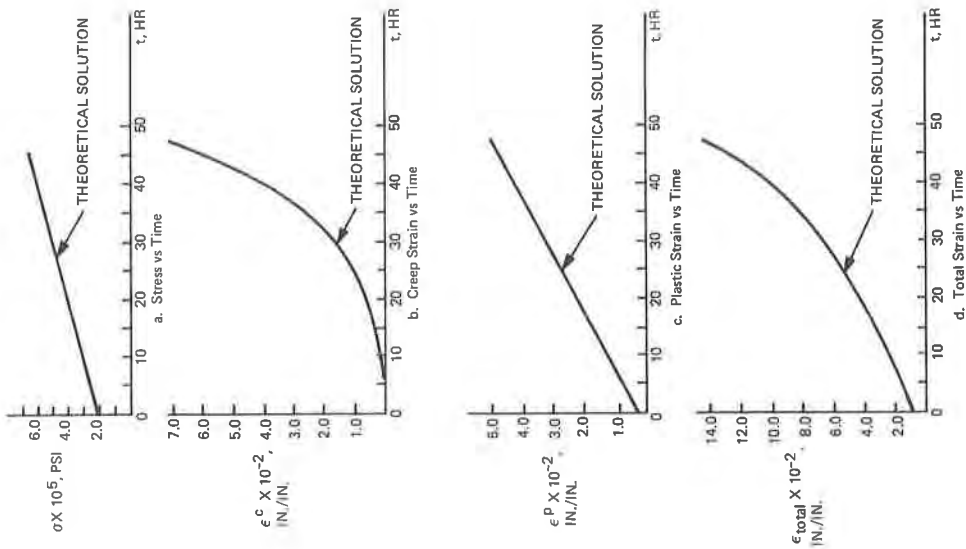


Fig. 3 - Stress and Strain vs Time for the Uniaxial Extension of a Rod with Time Varying Load Under Combined Plasticity and Creep Behavior

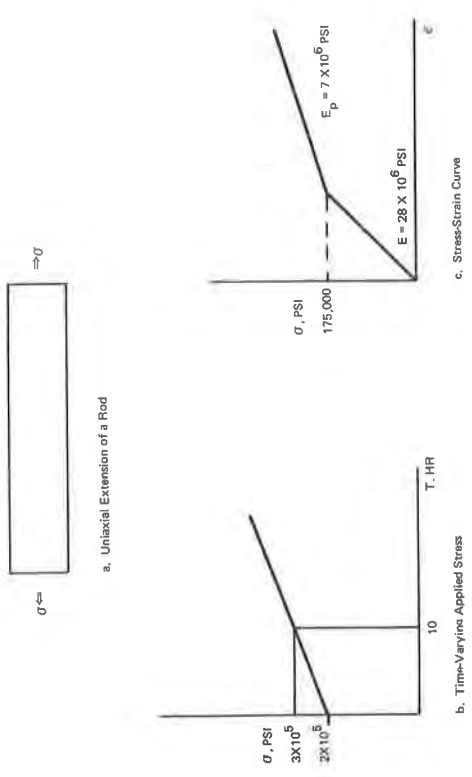


Fig. 2 - Uniaxial Extension of a Rod with a Varying Time Load under Combined Creep and Plasticity

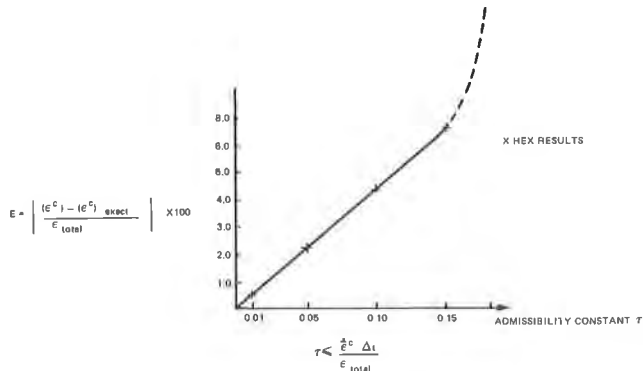


Fig. 4 - Creep Strain Error vs Admissibility Constant

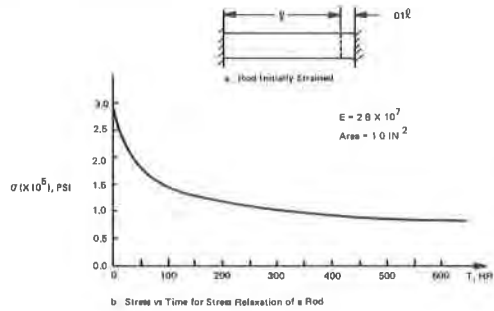


Fig. 5 - Stress Relaxation of Rod Under Initial Strain

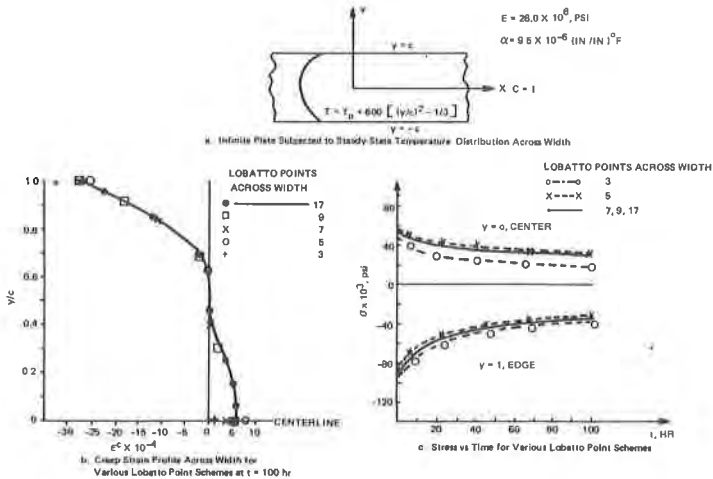
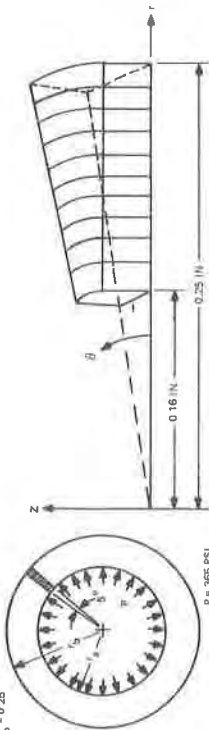


Fig. 6 - Thermal Stress Relaxation of a Plate

$$\nu_s = 0.16$$

$$\nu_b = 0.25$$



$$p = 365 \text{ PSI}$$

$$E = 2.8 \times 10^7 \text{ PSI}$$

$$\nu = 0.499$$

a. Internally Loaded Thick-Walled Cylinder

b. Ten Element Idealization

Fig. 7 - Finite Element Idealization of Thick-Walled Cylinder

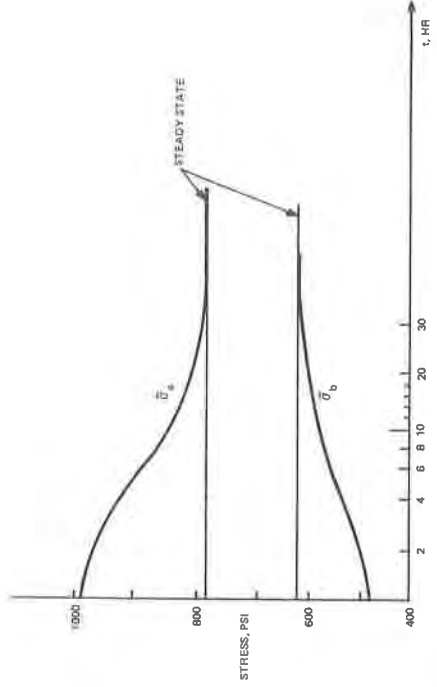


Fig. 8 - Stress-Time History for Internally Loaded Thick-Walled Cylinder ($\bar{\sigma}_r$ and $\bar{\sigma}_b$ Correspond to the Equivalent Stress at the Inner and Outer Radii, Respectively)

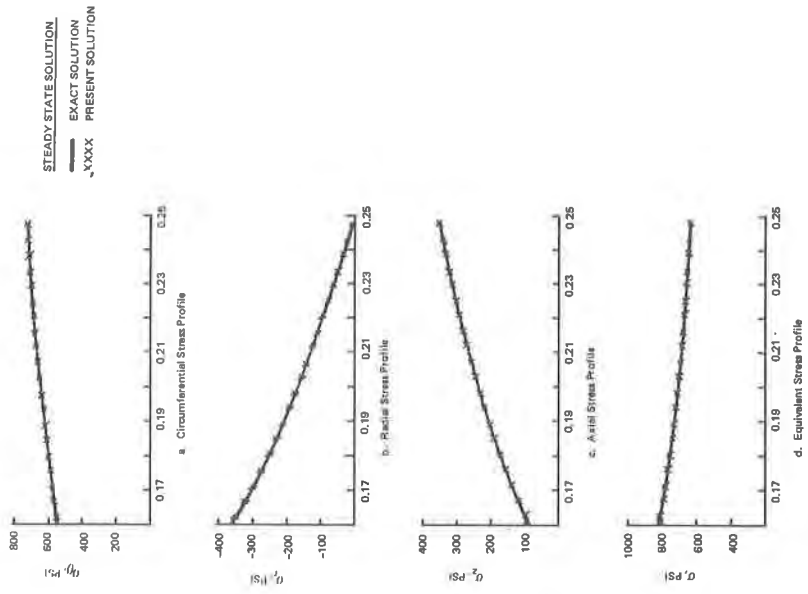


Fig. 9 - Steady-State Response to Internally Loaded Thick-Walled Cylinder